

Peter Neri and Dennis Levi

J Neurophysiol 102:2594-2602, 2009. First published Sep 2, 2009; doi:10.1152/jn.00489.2009

You might find this additional information useful...

This article cites 23 articles, 6 of which you can access free at:

<http://jn.physiology.org/cgi/content/full/102/5/2594#BIBL>

Updated information and services including high-resolution figures, can be found at:

<http://jn.physiology.org/cgi/content/full/102/5/2594>

Additional material and information about *Journal of Neurophysiology* can be found at:

<http://www.the-aps.org/publications/jn>

This information is current as of November 6, 2009 .

Surround Motion Silences Signals From Same-Direction Motion

Peter Neri^{1,2} and Dennis Levi²

¹Institute of Medical Sciences, Aberdeen Medical School, Aberdeen, United Kingdom; and ²School of Optometry and Helen Wills Neuroscience Institute, University of California, Berkeley, California

Submitted 4 June 2009; accepted in final form 27 August 2009

Neri P, Levi D. Surround motion silences signals from same-direction motion. *J Neurophysiol* 102: 2594–2602, 2009. First published September 2, 2009; doi:10.1152/jn.00489.2009. The response of motion-sensitive neurons to stimuli presented within their receptive field is often affected by stimulation in the surrounding region. These effects have perceptually relevant consequences that can be measured using behavioral techniques. We used psychophysical reverse correlation to characterize directional selectivity in human observers while they processed a local motion stimulus and studied the effect of adding an additional motion signal in the surrounding region. The surround had no effect on response gain for signals of opposite direction but selectively reduced gain for those of same direction. Surprisingly this reduction was close to 100%, effectively amounting to a gating process whereby signals of same direction were completely silenced. Our data indicate that by far the most prominent perceptual manifestation of center-surround antagonism is gain suppression by motion in the same direction without any appreciable change in directional tuning.

INTRODUCTION

Contextual influences on the processing of local motion signals have been extensively demonstrated in both single neurons and human observers (Allman et al. 1985). In single neurons, the spike response to a directional stimulus is strongly modulated by the presence of a surrounding motion stimulus (Born 2000; Cavanaugh et al. 2002). The most common finding is that surround motion reduces the response to motion in the same direction within the central part of the receptive field (Born and Bradley 2005; Pack et al. 2005). These neuronal effects are believed to underlie a variety of perceptual phenomena reported for human observers, most relevant here the reduction of contrast sensitivity for drifting stimuli above a certain size (Tadin et al. 2003).

Despite the extensive literature on surround effects in motion perception (Paffen et al. 2005; Tadin et al. 2005) and previous attempts at addressing some of the issues considered in the following text (Falkenberg and Bex 2007), it is not known exactly in what ways the surround modifies directional tuning: for example, does the surround reduce the overall response to motion uniformly across different directions or does it affect some directions more than others? Does the directional tuning curve change shape or does it remain more or less unaffected except for an overall scaling of its amplitude? To address these and other related questions, we derived directional tuning curves from human observers using a psychophysical variant of reverse correlation known as noise image classification (Ahumada 2002; Neri and Levi 2006) and compared the resulting curves for different surround stimuli.

Address for reprint requests and other correspondence: P. Neri, Institute of Medical Sciences, Aberdeen Medical School, Aberdeen, United Kingdom (E-mail: peter.neri@abdn.ac.uk).

Our main finding is that directional tuning curves around a given direction are mostly unaffected by surround motion in the opposite direction but are essentially abolished by surround motion in the same direction, meaning that the directional tuning curve becomes flat. This result appears to be a necessary consequence of the surround because we designed our stimuli so that the surround was clearly labeled as separate from the center target and it provided no useful information for the task at hand. Our results cannot be simply attributed to response bias or crowding. Taken together, our results can be parsimoniously interpreted in the context of a simple model based on the surround inhibition effects that have been reported for single neurons.

METHODS

Peripheral stimulus

The stimulus consisted of a sequence of frames like the one shown in Fig. 1A. Before and after the motion probe (detailed in the following text) “dots” were always present on the screen and never moved. The dots were anti-aliased Gaussian blobs (SD = 3.75 arcmin) with peak luminance of 74 (bright) or 0 (dark) cd/m² on a background luminance of 37 cd/m² (monitor was gamma-corrected). For regions where blobs overlapped, the pixel was assigned the luminance of the blob with the largest absolute value at that position. The motion probe lasted 300 ms, during which dots moved at 4.1°/s in different directions. We define two subregions for each side of fixation: the center (diameter: 2.1°, distance of center from fixation: 4.3°), corresponding to the circular region inside the red outline in Fig. 1A, and the surround (diameter: 7.6°), corresponding to the annular region between the red outline and the dashed outline in Fig. 1A. Within each center region a fixed percentage of the dots were signal dots, whereas the remaining dots were noise dots (different uncorrelated noise samples were used for left and right stimuli). Signal dots moved in opposite vertical directions within the two center regions: if signal dots moved upward within the region on the right (as in Fig. 1A), signal dots within the region on the left moved downward and vice versa. This “balanced” design enabled us to minimize the possible effects of response bias (see DISCUSSION). Each noise dot could take any of 16 directions (nearby directions differing by 22.5°) with uniform probability. There were 30 dots in total for each motion probe. Of these, 7.9 ± 2.8 (mean ± SD across observers) were signal dots. When dots reached the edge of the center region, they were wrapped around to the opposite side of the region along the same motion trajectory. Dots within the surround region moved in the same direction on both sides of fixation. Each trial could take any of the following three surround configurations (randomly chosen with equal probability on every trial): 1) no moving surround, i.e., surround dots remained static; 2) upward moving surround; and 3) downward moving surround. When surround dots moved, they did so at 4.1 deg/s.

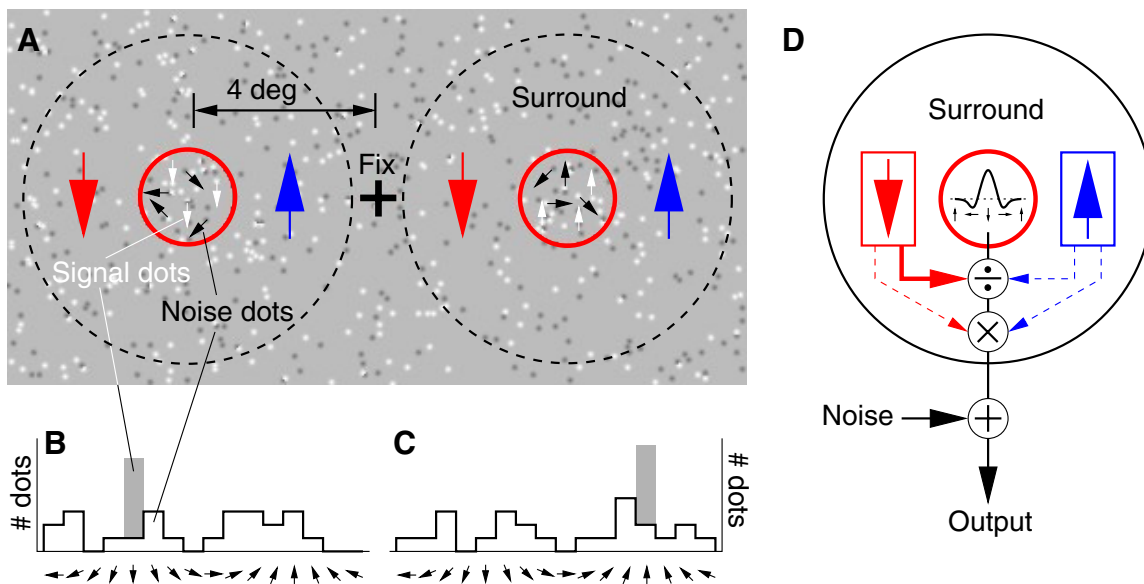


FIG. 1. **A**: 1 frame of the visual stimulus. Two center-surround stimuli appeared on each side of fixation. Each stimulus was divided into center (indicated by red outline) and surround (indicated by dashed line). The two red circles were actually present in the stimulus (but not the dashed circles). The center region contained a number of “signal” dots (white arrows), all moving in the same direction, and a number of “noise” dots (black arrows), all moving in random directions. Signal dots moved upward on one side of fixation and downward on the other side. Observers were asked to indicate which side moved downward. In the example shown here, it is the left side. **B** and **C**: the number of dots moving in different directions for both stimuli. Shaded histograms refer to signal dots, the remaining distribution to noise dots. Noise distributions were used to compute directional tuning functions for the human observers using psychophysical reverse correlation (see METHODS). **D**: schematic of the potential mechanisms underlying surround effects. In principle, the surround may cause inhibition (\div) or facilitation (\times) of center motion, and this effect may or may not depend on the direction of the surround [same (red) as center or opposite (blue) to center]. We only consider multiplicative effects because subtractive/additive effects cancel out in our 2-alternative forced-choice task (2AFC) paradigm (see DISCUSSION). Our results are consistent with only 1 of the 4 possible effects considered in the figure: same-surround inhibition (solid red arrow). All other effects (dashed arrows) are not supported by our data. We implemented this mechanism within a simple model (see METHODS) that was then used to replicate the human data (Fig. 2A).

Peripheral task

Observers were instructed to fixate the central cross and, following each trial, to press one of two buttons to indicate which of the two possible signal configurations were presented: either signal dots moved upward within the region on the left and signal dots moved downward within the region on the right or signal dots moved downward within the region on the left and upward within the region on the right. Their response triggered the next presentation after a random interval uniformly distributed between 150 and 300 ms. This task was worded in the following terms: press 1 for left or 2 for right to indicate the side where predominantly downward motion was seen, being aware that the other side always contains upward motion (“downward” was replaced with “upward” for half the observers). Performing this task requires access to directionally tuned mechanisms as both left and right stimuli contained the same amount of coherent (signal) and incoherent (noise) motion: a nondirectional motion detector that simply detects coherent motion along any direction would generate chance performance. Similarly motion streaks, which differ between coherent and incoherent motion (Edwards and Crane 2007), are not useful for performing this task because they lack directional information. Observers were initially familiarized with the task by presenting them with 20–30 trials containing 100% signal dots. They learned the task very quickly, after which we proceeded to vary the percentage of signal dots according to a 2-up 1-down staircase until their performance was around threshold (75% correct responses). The data shown here were collected at a fixed threshold number of signal dots (detailed earlier). Observers were explicitly instructed to ignore motion outside the center regions that were clearly outlined in red. We collected an average of $\sim 3,500$ trials per observer ($\times 6$ observers). Feedback (correct/incorrect) was provided after each response. All participants were naïve regarding the methodology and purpose of the study except for *S3* (author PN).

Foveal stimulus

Identical to the peripheral stimulus except for the following: 1) instead of presenting a stimulus on the left and one on the right of fixation, they were presented in temporal succession (0.5-s inter-stimulus gap) and centered at fixation; 2) the center region was much smaller (0.31° diam), which we achieved by a combination of reduced physical stimulus size and increased viewing distance (228 cm as opposed to 57 cm for peripheral viewing); 3) the surround region was also smaller (2.1° diam); 4) the center contained 12 dots, of which 4.6 ± 1.7 were signal dots; and 5) dot speed was reduced to $1^\circ/s$.

Foveal task

Identical to the peripheral task, except observers were now asked to choose between intervals 1 and 2 rather than between left and right sides of fixation (we opted for this design because it allowed us to use a center-surround configuration that was almost identical between peripheral and foveal conditions). We collected an average of ~ 800 trials per observer ($\times 10$ observers). All participants were naïve except for *S3*.

Derivation of perceptual filters

The stimulus presented within each circled region on each trial i can be described as $N_i(d)$, the number of noise dots that moved in direction d . If $N_i^t(d)$ refers to the region containing signal dots moving in the target (t) direction and $N_i^{nt}(d)$ refers to the other region (where signal dots moved in the opposite nontarget direction), then $\Delta N_i^c = N_i^t - N_i^{nt}$, where $c = 0$ if the observer responded incorrectly on trial i and $c = 1$ if the response was correct. The perceptual filter is computed as $P(d) = \langle \Delta N_i^1 \rangle - \langle \Delta N_i^0 \rangle$ where $\langle \rangle$ is used to indicate the mean across trials i (see Abbey and Eckstein 2002). In Fig. 2, this rule means that

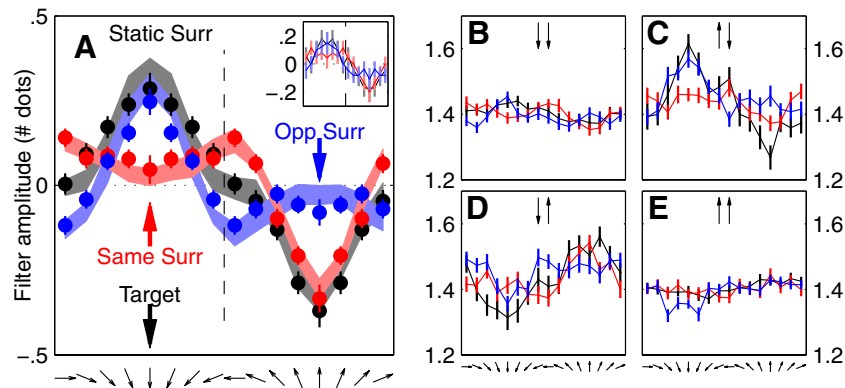


FIG. 2. Directional tuning curves for the aggregate observer. Black refers to trials where the surround was static, red to trials where the surround moved in the target direction (indicated by the label “target”), and blue to trials where the surround moved in the direction opposite to the target. A: sensory filters derived from all noise fields and all trials (see METHODS) for both peripheral (main panel, total of 21,200 trials) and foveal experiments (top right inset, total of 8,057 trials). B–E: averages of noise fields from correct (B and E) and incorrect (C and D) trials separately as well as downward-moving (B and D) or upward-moving signal dots (C and E) separately (only data from the periphery shown). These different subclasses are coded by the small black arrows at the top of each panel: left arrow indicates the direction of the signal dots within the stimulus of interest, right arrow indicates the direction reported by the observer for that stimulus. The combined trace in A was computed by adding B and C and subtracting D and E as well as symmetrically averaging directions off vertical and horizontal (see METHODS and RESULTS). Error bars show ± 1 SE. Shaded regions show simulated tuning curves (± 2 SD) for a simple model where the surround silences the output from filters preferring the same direction (see METHODS).

$A = (B + C) - (D + E)$ where letters refer to panels. For the spatial distribution analysis (Fig. 5), we subdivided the center region of the stimulus into five annuli of equal area (diagram in Fig. 5A) and derived perceptual filters separately for each annulus. We then computed the root-mean-square overall modulation of the tuning function for each annulus as $\sqrt{P(d^2)}$ where \diamond is used to indicate mean across d . Dots were assigned to the annulus where they appeared half-way through their motion trajectory.

Directional gain

If f^s is the directional tuning function for static surround, and f^m for moving surround, directional gain g is defined as $f^m = g \times f^s + s$, i.e., it is the slope of the best-fitting line (Neri 2006; Treue and Martínez-Trujillo 1999).

Estimation of human consistency

We performed a series of double-pass experiments in which the same set of stimuli is presented twice and the percentage of same responses to the two sets (termed consistency) is computed (Neri and Levi 2006). We ran 100-trial blocks (like in the main experiment) during which observers were not aware of any difference with respect to blocks for the main experiment. In double-pass blocks, the second half of 50 trials showed the same stimuli presented during the first half of 50 trials but in randomly permuted order. Consistency, in combination with percentage correct, can be used to estimate internal noise in units of external noise SD provided certain assumptions about the underlying statistics and a signal detection model of observer choice (see Burgess and Colborne 1988 for details). We collected an average of ~ 480 trials per observer. We were only able to perform these measurements on a subset of our original sample (3 observers for the peripheral condition and 8 for the foveal condition) because some observers were unavailable at the time we carried out the double-pass experiments.

Modeling

$S_i^s(d)$ refers to the stimulus (signal + noise) within the region containing the target t (30 dots of which 8 were signal dots as for average of the human observers). The output of the preferred-direction receptive field (RF) for this stimulus is $o_i^p = S_i^s(d) \cdot f^p(d) + \varepsilon$, the dot product with the preferred (same as target) direction filter $f^p = k^p G(d')$

plus an internal Gaussian noise source (SD 0.057 based on piloting). Similarly for o_i^a , the output of the antipreferred-direction RF $f^a = k^a G(d'')$. $G(\mu)$ is an even Gabor function centered on direction μ (d' is target direction and d'' is nontarget direction) with 67.5° SD for the Gaussian envelope and 225° period of the sinusoidal carrier (shown in Fig. 1D). The response to the stimulus is simply $r_i^t = o_i^p - o_i^a$ (neuron/antineuron decision variable). The model responded correctly on trial i when $r_i^t > r_i^{nt}$ (where r_i^{nt} is the response to the stimulus containing the nontarget) and incorrectly otherwise. Gain constants k^p and k^a were both set = 1 to simulate the static surround condition. When the surround moved in the target direction, $k^p = 0$ and $k^a = 1$; when in the nontarget direction, $k^p = 1$ and $k^a = 0$.

RESULTS

Overall shape of the directional tuning functions

Observers were asked to select one of two stimuli that appeared on opposite sides of fixation (spatial 2-alternative forced choice). Both stimuli contained moving dots within a circular region (indicated by red circle in Fig. 1A), a percentage of which were noise dots, whereas the remaining ones were signal dots. In the target stimulus (Fig. 1, A, left, and B), noise dots moved in random directions, whereas signal dots all moved downward. The nontarget stimulus (Fig. 1, A, right, and C) was the same except the signal dots moved upward. Observers were asked to report which side contained the target (left in the example shown in Fig. 1). We then applied psychophysical reverse correlation to recover directional tuning functions, an example of which is shown by the black data points in Fig. 2A for the aggregate observer (see METHODS and Fig. 2, B–E, for details on how different noise fields were combined to obtain the tuning function shown in A). We symmetrically averaged directions off vertical and horizontal (i.e., we averaged $\uparrow + \pi/8$ with $\uparrow - \pi/8$, $\uparrow + \pi/4$ with $\uparrow - \pi/4$, $\uparrow + 3\pi/2$ with $\uparrow - 3\pi/2$, $\downarrow + \pi/8$ with $\downarrow - \pi/8$, $\downarrow + \pi/4$ with $\downarrow - \pi/4$, $\downarrow + 3\pi/2$ with $\downarrow - 3\pi/2$) because (as expected) no significant asymmetries were observed. In line with our previous work (Neri and Levi 2008a), there is a positive peak at target direction and a negative peak at the opposite (nontarget) direction.

We repeated this measurement in the presence of a moving surround (the extent of which is indicated by dashed circles in Fig. 1A). The surround moved in the same direction on both sides of fixation. On different trials, this could be the target direction (red arrows in Fig. 1A) or the nontarget direction (blue arrows). As shown by the red and blue data points in Fig. 2, the presence of the surround substantially modified the resulting directional tuning functions. More specifically, directional tuning is flattened within the region corresponding to the direction of the surround. This is the main finding of the present study.

There is an obvious symmetric structure in Fig. 2, which is not surprising given the symmetry of the task itself. Because both target and nontarget contained a signal and because it took opposite directions in the two stimuli, it is reasonable to expect that observers used two motion detectors to perform the task: one selective for the direction of the target and one selective for the direction of the nontarget. The final response would be based on the difference between the outputs from the two detectors, thus generating a directional tuning curve where the right-hand side (centered on the nontarget direction) is an inverted image of the left-hand side (centered on the target direction), as observed for the black data points in Fig. 2. Similarly, we expect that the two types of surround we used would impact the directional tuning curves in such a way that the right-hand side for one surround type (e.g., blue trace) would be an inverted image of the left-hand side for the other surround type (e.g., red trace), as we observed for red and blue data points in Fig. 2.

We exploited this symmetry in Fig. 3A (*main panel*), which was obtained from the data in Fig. 2A. More specifically, the black trace in Fig. 3A was obtained by averaging left- and right-hand sides of the black trace in Fig. 2A, after inverting the sign of the right-hand side. The blue trace was obtained by averaging the left-hand side of the blue trace in Fig. 2A with the right-hand side of the red trace in Fig. 2A, after inverting the sign of the latter. Finally, the red trace was obtained by averaging the left-hand side of the red trace in Fig. 2A with the right-hand side of the blue trace in Fig. 2A, after inverting the sign of the latter. Notice therefore that although black in Fig. 3A is directly related to black in Fig. 2A, the red and blue traces in Fig. 3A were obtained by mixing the red and blue traces in Fig. 2A so the correspondence is not immediate.

The small panels next to Fig. 3A show individual data for the six different observers (after symmetric averaging). We found a significant degree of variability across observers, making it difficult to draw conclusions from simply inspecting individual directional functions. For this reason, we performed additional analyses that captured the main features of these functions and quantified each feature using a single value for each perceptual filter. This enabled us to perform simple population statistics in the form of paired *t*-test across observers and confirm or reject specific hypotheses about the overall shape of the directional functions. Note that our analyses are 1) based on raw data, not on smoothed data and 2) based on individual observer analysis, not on observer averages. These issues are very relevant to noise image classification analysis because there is no generally accepted way of averaging data across observers, and any such averaging scheme is subject to pitfalls (see Neri and Levi 2008b for a detailed discussion of this issue).

Surround effects on directional gain

The data in Fig. 3A can be summarized as follows: the surround has little effect on directional tuning in the opposite direction (blue trace) but essentially abolishes tuning in the same direction (red trace). To capture this effect, we measured the multiplicative scaling factor that is applied to the black trace to obtain the other two traces. This quantity is termed directional gain (see METHODS) and is plotted in Fig. 4A, where gain for the blue traces in Fig. 3 is plotted on the *x* axis, whereas gain for the red traces in Fig. 3 is plotted on the *y* axis. No effect corresponds to gain = 1. Data points for individual observers (black open symbols) show that directional gain was not different from 1 (*t*-test $P = 0.44$) for directional tuning in the direction opposite to the surround (blue traces in Fig. 3) but was significantly smaller than 1 ($P < 0.005$) for directional tuning in the same direction as the surround (red traces in Fig. 3). Both effects are clear for the aggregate observer, indicated by the solid black symbol in Fig. 4A: this point falls near the vertical dashed line (gain = 1 for opposite direction) and near the horizontal solid line (gain = 0 for same direction).

The visible spread in Fig. 4A shows that as previously noted, we found significant variability across observers. Can these differences stem from individual task strategies? We think this unlikely. First, we did not find significant bias for one side of the display over the other in the peripheral experiments [$P =$

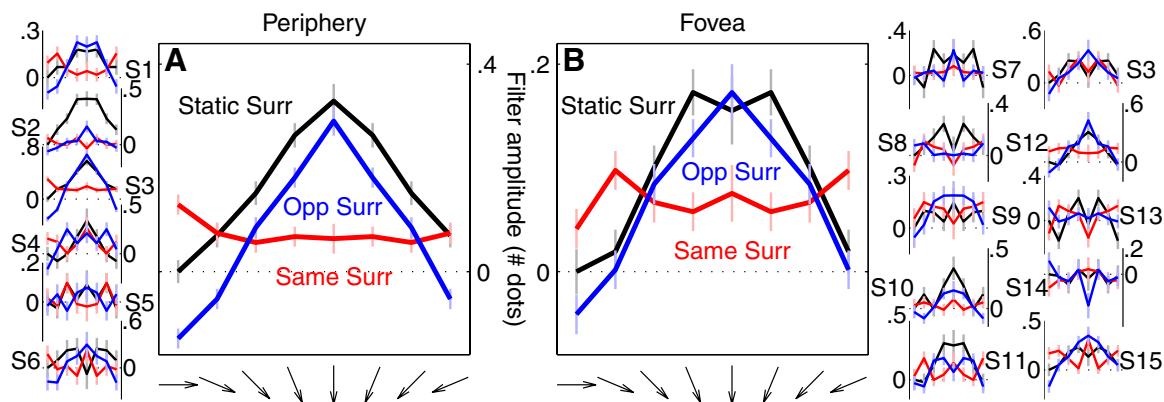


FIG. 3. Symmetrically averaged directional tuning curves. The obvious symmetry in Fig. 2A (also expected from stimulus and task design, see main text) was exploited to obtain directional tuning curves ranging $\pm 90^\circ$ around target direction (see *x* axis). Color coding as in Fig. 2. A: aggregate data for the periphery; B: aggregate data for the fovea. Small panels show data for individual observers (*left*: periphery; *right*: fovea).

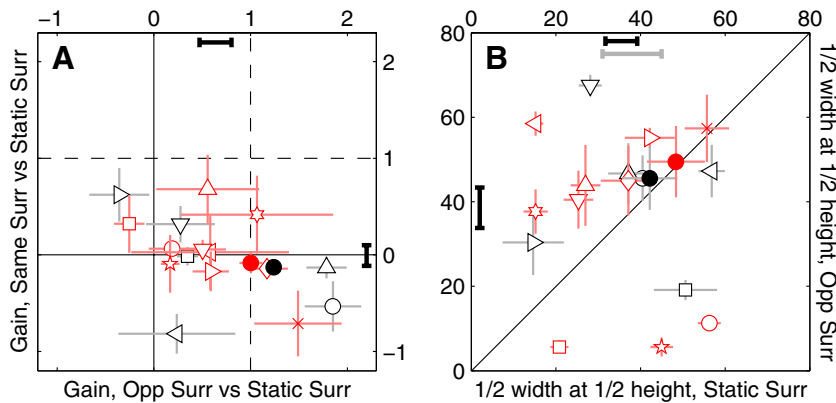


FIG. 4. Directional gain and half-width at half-height. *A*: directional gain (see METHODS) is plotted for the surround moving in the target direction (*y* axis) vs. the surround moving in the opposite direction (*x* axis). Black symbols: peripheral data; red symbols: foveal data. Open symbols: individual observers (1 data point per observer with different symbols referring to different observers); solid symbols: aggregate observer. Bars next to axes show mean \pm SD across all data points (excluding aggregate). *B*: half-width at half-height of the directional tuning functions is plotted for the surround moving in direction opposite to target (*y* axis) vs. static surround (*x* axis). Plotting conventions as in *A*. Gray bar next to top *x*-axis shows estimate from Neri and Levi (2008a).

0.28 for percentage of “left” responses different from 0.5 (*t*-test) across observers], nor for one interval over the other in the foveal experiments ($P = 0.53$). Second, the spread is very similar for foveal and peripheral data despite the fact that most of the observers in the peripheral experiments were experienced in psychophysical testing (although naïve about the purpose of the experiments), while most of the observers in the foveal experiments were inexperienced. Third, a similar degree of spread was observed for both surround directions (compare *x* and *y* axes); this, combined with the above considerations, suggests to us that the variability we observed most likely reflects measurement noise.

Surround effects on directional tuning

Although the presence of the surround had no measurable effect on directional gain for the opposite direction, it may have modified directional tuning, i.e., the blue trace in Fig. 3*A* may be broader or narrower than the black trace. To test this possibility, we measured half-width at half-height for the black traces in Fig. 3*A* and plotted them on the *x* axis in Fig. 4*B* versus the same measure for the blue traces on the *y* axis (width is appropriately defined as half-width at half-height after rescaling the curve to its maximum and minimum values; see McAdams and Maunsell 1999 for why this is the correct way to calculate width). The surround had no significant effect on tuning width (paired *t*-test $P = 0.64$), i.e., black symbols fall on the diagonal unity line. We conclude that the presence of the surround had no effect on directional tuning for the opposite direction in the same way that it did not affect gain. It was not possible to carry out the same analysis on directional tuning for

the same direction as the corresponding directional tuning curves (red traces in Fig. 3*A*) were too flat to yield any reliable estimate of width. Finally, the width estimates reported here overlap closely with our independent estimate from previous work (Neri and Levi 2008a) indicated by the gray bar in Fig. 4*B*.

Spatial distribution of gain reduction

The directional tuning functions examined so far were derived from all the noise dots within the circular target region (red circles in Fig. 1*A*). However, it is possible that observers were processing only dots closer to the edge or closer to the center of this region and/or that the effect of the surround was most pronounced for the former than for the latter (or vice versa). To study the spatial distribution of these effects within the circular target region, we derived directional tuning functions for dots within different annuli centered on the stimulus (diagram in Fig. 5*A*) and computed the overall modulation of the tuning function for each annulus (see METHODS).

Figure 5*A* shows modulation for different annuli, from center (indicated by 0 on the *x* axis) to edge (indicated by 4 on the *x* axis). There was a small effect of larger modulation within the central annulus (black trace), but it was not significant across observers. In general, we found that modulation was more or less uniform across the target region. We then focused on the effect of same-direction surround, shown in Fig. 5*A* by the gray trace. The aggregate data suggest that gain reduction by same-direction surround may be more pronounced within the central annulus than at the edge (compare black with gray trace). We therefore analyzed this effect further by taking the ratio between modulations with moving

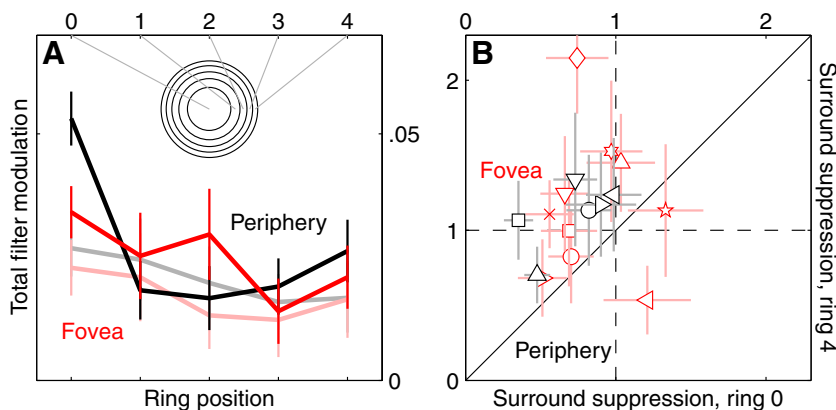


FIG. 5. Spatial distribution of surround suppression. *A*: plot of filter modulation (root mean square of directional tuning function, see METHODS) for different annuli of equal area within the center region of the stimulus. Full colors for static surround, light colors for surround moving in target direction. *B*: plot of surround suppression (ratio between light-colored and full-colored values from *A*) using the same conventions as in Fig. 4, for the outermost annulus (*y* axis) vs. the innermost annulus (*x* axis).

surround (gray) and those with static surround (black). Figure 5B plots this modulation ratio for the central ring (0) on the x axis versus the edge ring (4) on the y axis, for all observers (open black symbols). Although there was a significant degree of variability across observers, the modulation ratio for ring 0 was significantly smaller than for ring 4 (black points fall above the unity line, paired t -test returns $P < 0.01$). This result suggests that the effect of gain reduction by the surround was most pronounced within the central region of the target stimulus or possibly only present within this region given that modulation ratios were different from 1 for ring 0 (points fall to the left of vertical dashed line, $P < 0.05$) but not for ring 4 (points fall on the horizontal dashed line, $P = 0.28$).

Surround effects on overall performance

As expected from the task symmetry discussed earlier, the percentage of correct responses (% correct) was similar for both directions of the surround: this quantity is plotted in Fig. 6A on different axes for the two directions, and black points fall on the unity line ($P = 0.1$). We therefore averaged the two values, and plotted them on the y axis in Fig. 6B versus percentage correct for static surround on the x axis. Clearly, the presence of a moving surround significantly reduced performance (black points fall below the unity line, $P < 0.02$).

We were also interested in whether learning occurred during the experiments, particularly because it is conceivable that the effect on performance caused by the moving surround may have diminished as observers learned to perform the task more efficiently. Figure 6C plots percentage correct for 20 different epochs across observers (we first computed 20 values for each observer by dividing his/her dataset into 20 sequential chunks containing the same number of trials each and then averaged the 20 values across all observers). There was a modest degree of learning, both for static (solid) and moving (open) surround: linear fits (solid black line for static surround and dashed line for moving surround) return a positive slope, but the effect is small. Importantly, the difference in performance between the two conditions was present throughout data collection. Note that our choice of SNRs delivered an optimal range of performance for noise image classification (Murray et al. 2002) (75% is indicated by the horizontal dotted line).

Surround effects on internal noise

Some aspects of our results may be explained by a nonspecific increase in task difficulty: for example it may be that observers are put off by the disruption caused by a moving surround and respond more randomly on those trials. The surround would then cause observers' responses to be decorrelated with the dot motions in the stimulus; this may explain the drop in performance detailed in the previous section (and documented in Fig. 6). This hypothesis can also be rephrased as an increase in system internal noise, which may lead to a reduction in the gain of the derived sensory filters (Ahumada 2002) although it does not explain why we did not observe a similar reduction for both same and opposite directions (see DISCUSSION).

To address this issue with data, we performed a series of double-pass experiments where observers were presented with the same stimulus twice (see METHODS). The percentage of trials on which they give the same response to both presentations of the same stimulus is termed consistency (Neri and Levi 2006) and provides an indirect measure of late additive internal noise (Burgess and Colborne 1988). Figure 7 plots both consistency (A) and estimated internal noise (B) for trials on which the surround was static (x axis) versus trials on which it was moving (y axis; we averaged values from the two surround types as they did not differ significantly in line with the percentage correct result shown in Fig. 6A). Data points fall on the unity line ($P = 0.17$ for the data in Fig. 7A and $P = 0.57$ for B), demonstrating that there was no detectable change in internal noise due to the moving surround.

Foveal data

All the data presented so far was collected in the periphery. A relevant question is whether the same effects apply to the fovea as there are important differences between these two neural structures in relation to several phenomena, particularly crowding. Crowding is strong and extensive in peripheral vision and weak or absent in the fovea (Levi 2008). We therefore repeated our experiments in the fovea using a two-interval forced-choice (2IFC) protocol [instead of the 2-alternative forced-choice task (2AFC) protocol used for the periphery]. Apart from a few relatively unimportant differences, the

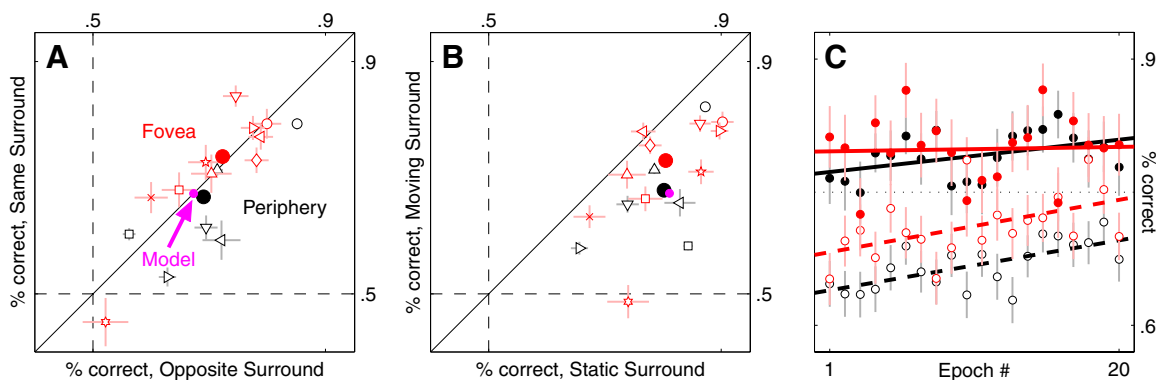


FIG. 6. Performance is impaired by the moving surround. A: percentage of correct responses (2AFC task) for surround moving in target direction (y axis) vs. surround moving in opposite direction (x axis). Same plotting conventions as Fig. 4. Magenta refers to simulated performance for the gain control model (see METHODS). B: percentage of correct responses for both surround types (average) vs. static surround (x axis). C: performance for 20 different epochs throughout data collection (averaged across observers, see main text). Black: periphery; red: fovea. Solid symbols and lines (best linear fits): static surround; open symbols and dashed lines: moving surround.

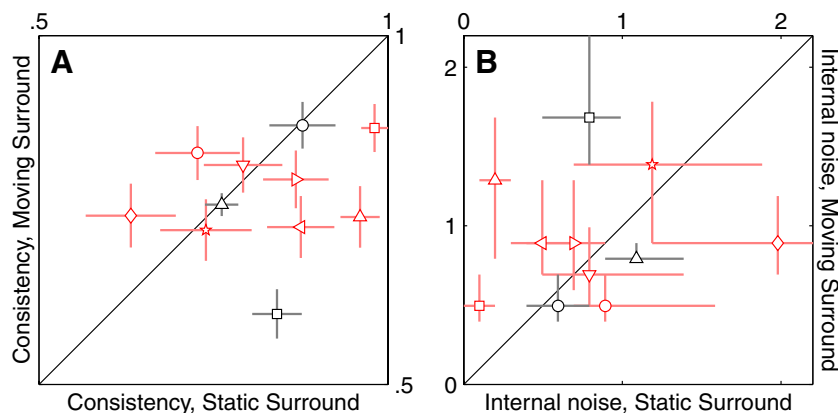


FIG. 7. Internal noise is not significantly affected by the moving surround. *A*: consistency (percentage of same responses to repeated presentation of the same stimulus) for moving surround (y axis) vs. static surround (x axis). Data for the moving surround show the average between the 2 surround conditions as they did not differ significantly. Same plotting conventions as Fig. 4. *B*: internal noise for moving surround (y axis) vs. static surround (x axis), same plotting convention as *A*. Internal noise is in units of external noise SD and is estimated by combining consistency (plotted in *A*) with percentage correct (Fig. 6) under specific assumptions (Burgess and Colborne 1988) (see METHODS).

results were essentially identical to those obtained in the periphery [compare *A* (periphery) with *B* (fovea) in Fig. 3 and black symbols (periphery) with red symbols (fovea) in Figs. 4–7]. The only difference was in relation to the spatial distribution of surround inhibition. While we found a degree of anisotropy for the peripheral targets (detailed in the preceding text), no significant anisotropy was found for the fovea (red points are not significantly above the unity line in Fig. 5*B*, $P = 0.1$). However, this spatial analysis did not show any significant effect of surround inhibition at all (red points are neither significantly below the horizontal dashed line ($P = 0.29$), nor significantly to the left of the vertical dashed line ($P = 0.1$) in Fig. 5*B*). It is therefore possible that when the foveal data were split into different target subregions, the amount of data per subregion did not carry sufficient statistical power and potentially existing effects may have gone undetected.

DISCUSSION

Compulsory nature of surround effects

We designed our experiments to maximize the potential for observers to ignore the surround. First, observers were explicitly instructed to do so and were told that the surround provided no useful information for performing the task (this was obvious anyway because surround motion was the same on both sides). Second, the surround was clearly demarcated from the center by a red outline (see Fig. 1*A*): there was no ambiguity as to which part of the display was relevant (center) and which was irrelevant (surround). Third, the overall design was fully symmetric, thus minimizing response bias. Our study differs methodologically from previous studies mainly in relation to these three issues. Below we focus primarily on the work of Tadin et al. (2003, 2006) because it is so directly relevant to our study, but other investigators reported results that are broadly consistent with our findings (e.g., Falkenberg and Bex 2007; Paffen et al. 2005).

Tadin et al. (2003) showed that sensitivity drops as the size of a high-contrast, foveally presented moving Gabor is increased. This result provides indirect evidence for surround inhibition, and our own results (as well as Tadin et al. 2006) support this finding. However, in Tadin et al. (2003), the entire stimulus provided useful information for performing the task, thus observers may have attended to its full extent when producing the psychophysical response. There was no explicit distinction between center and surround either in the stimulus

or in the instructions given to the observers. It remains possible that had observers been instructed to ignore the stimulus outside a clearly defined region, their sensitivity would not have dropped with stimulus size in the experiments of Tadin et al. (2003). Our experiments were designed, among other things, to address this question directly. Our results indicate that, at least for the stimulus parameters we tested, the surround could not be ignored despite being clearly labeled (Fig. 1*A*), explicitly presented to the subjects as irrelevant and to be ignored and detrimental to their performance (Fig. 6*B*) under trial-by-trial feedback conditions. Moreover, the deleterious effect of the surround persisted over thousands of trials (Fig. 6*C*).

In a subsequent study, Tadin et al. (2006) manipulated center and surround independently. Similar to us, they found that the surround affected performance despite the fact that observers could potentially ignore it. A technical issue with their study is that they used a one-interval direction discrimination task (not a 2AFC task). In general, their design would not be subject to bias because observers can be assumed to show no preference between left- and rightward motion. In the presence of a directional surround, however, this assumption may not be valid. For example, it is conceivable that when the surround is predominantly moving leftward, observers may be biased toward reporting leftward (or rightward) motion, and this could in turn lead to an apparent drop in sensitivity. We are not suggesting that this was the case. In fact our data support their results and indicate that it probably was not, but this is potentially an issue that needed clarification. Our design excludes bias of this kind. If observers were biased to report downward over upward (or vice versa) when the surround was moving downward, this bias would apply equally to both stimuli on both sides of fixation, factoring out bias in their final response.

Gating of same-direction signals by the surround

The most significant effect induced by the moving surround was the gain reduction for directional signals tuned to the same direction as the surround itself (Fig. 2*A*). The gain reduction is not particularly surprising given existing electrophysiological evidence (Allman et al. 1985; Born and Bradley 2005); however, the quantitative extent of the reduction is surprising: gain is not simply reduced, it is silenced (Fig. 4*A*). As a consequence, the tuning curves are flat and directional tuning is abolished (Figs. 2 and 3). Such a pronounced gain reduction is

rarely observed in single neurons, so the perceptual read-out must take place after a threshold nonlinearity is applied along the sensory processing pathway. Alternatively, suppression may not have been complete, but our measurements were unable to resolve the residual gain signal; we cannot exclude this possibility as our experiments are obviously limited in the amount of data we can collect. What we can say is that suppression was strong enough that, given the resolution of our measurements and experimental protocols, it was indistinguishable from complete suppression.

To illustrate our interpretation of the results, we implemented the simplest possible model that could account for our results. In this model, motion signals within the stimulus center are linearly weighted by the preferred directional filter shown in Fig. 1D (inside the red circle) as well as by the anti-preferred filter (i.e., preferring the opposite direction). The difference between the outputs from the two filters is the response to the center (after the addition of late additive internal noise, see METHODS). This procedure is applied to both left and right stimuli. The stimulus associated with the largest response is chosen as the target. When the surround is static, preferred and anti-preferred filters have equal gain. When the surround moves, the gain of the filter that prefers the direction of the surround is set to 0. We challenged this model with the stimuli used for the human observers and derived the associated sensory filters, indicated by shaded regions in Fig. 2. It is clear that the model captures the experimental results remarkably well, not just in the shapes of the tuning curves but also in relation to performance (magenta points in Fig. 6, A and B).

It must be emphasized that our model involves divisive and not subtractive inhibition: if the response of a directional filter is $g \times f + s$ (where f is a normalized tuning function, g is gain, and s is baseline response), our model involves a change in g not s (see METHODS). Subtractive effects are immaterial to our 2AFC design: if the surround subtracts a signal from the center, it will do so equally on both intervals. Because the final decision is based on the relative difference between the responses to the two intervals, any subtractive effect cancels out and does not affect the final choice made by the observer (similarly to bias). This distinction bears on the possibility that induced motion played a role in our experiments. In the context of our model, induced motion would involve an additive increase of the response for the induced filter (a change in the value of s) and possibly a subtractive decrease of the response for the opposite-direction filter. These effects may be operating under the conditions of our experiments, but our protocol does not allow us to measure them, and most importantly they do not explain our results as they predict no effect on gain. A similar logic applies to a potential role for eye movements in our experiments: if the effect of eye movements is modeled as induced motion, it plays no net role in our experiments. Additionally we note that our stimuli were relatively brief ($<1/3$ s) so as to minimize a potential role for eye movements, and that our results were very similar between fovea and periphery despite significant differences in stimulus configuration and AFC design (spatial vs. temporal). Eye movement patterns may be expected to differ significantly between the two sets of experiments, yet we observed no difference in the overall results.

An interesting feature of the model is that the late additive noise source was never changed, i.e., the presence of the

surround was modeled as only affecting the amplitude of filter outputs, not their internal noise [however, the introduction of internal noise was necessary for an accurate simulation of the results ranging from the details of the directional tuning functions (Fig. 2A) to overall performance (Fig. 6, A and B)]. The issue of internal noise relates to the possibility that our results may be explained by the moving surround causing observers' responses to be decorrelated with the dot motions in the stimulus, as already discussed in RESULTS. Our simulations indicate that this is unlikely. Furthermore, aside from the modeling considerations, we can exclude this interpretation based on the result that although there was a complete gain reduction for same-direction motion signals (which in principle may be consistent with complete decorrelation of observers' responses), there was no concomitant change in gain for the opposite direction. Because directional filters were derived from the same noise fields on the same trials, simple response decorrelation would predict a significant gain reduction for both motion directions, contrary to what we observed. Finally, we empirically estimated late internal noise using a double-pass technique (see METHODS) and confirmed that this source of decorrelation was not affected by the moving surround (Fig. 7).

One aspect of the model appears inconsistent with existing evidence, namely the Mexican-hat shape of the front-end directional filter (Fig. 1D). Most MT neurons present a unimodal directional tuning function (Born and Bradley 2005), and previous psychophysical estimates of directional tuning using reverse correlation do not show negative side-flanks (Busse et al. 2008; Murray et al. 2003; Neri and Levi 2008). With relation to the psychophysical findings, previous studies may have failed to expose the negative flanks for the same reason that our own data and model fail to show them when both preferred and anti-preferred filters have equal gain (black trace in Fig. 2): the flanks are masked by overlapping profiles from the two opposite directions (they cancel each other out). The flanks are exposed here because we silenced one of the two filters via surround inhibition, allowing us to measure the other filter in isolation. With relation to the physiology, we speculate that the sensory filter we estimated psychophysically may derive from the combination of two unimodal tuning functions with different degrees of directional tuning, the less-tuned subtracted from the more finely tuned in the fashion of a difference-of-Gaussian (DOG) model. This interpretation allows us to reconcile the present findings with the tuning functions recorded from single neurons in MT, but there is no evidence to either prove or disprove it at this stage. Alternatively, because Mexican-hat directional tuning has been reported across the V1 neuronal population [see Fig. 3D in Cavanaugh et al. 2002], it is possible that our data may simply reflect the properties of a neuronal subpopulation within V1.

Spatial spread of the surround effects

Perhaps unexpectedly, we found that surround inhibition was more pronounced for signals in the middle of the center target and almost absent for those at the edges (Fig. 5). Because the latter are closer to the surround, we expected a larger effect at the edges, opposite to what we observed. However this expectation is based on the assumption that the point-spread function for inhibition (i.e., the amount of inhibition delivered by each point in visual space to the surrounding region) peaks

at the origin (e.g., 2D Gaussian), which is unlikely. A more realistic point-spread function would deliver little inhibition at the origin (corresponding to self-inhibition), peak at some distance away from the origin, and then peter out again for larger distances. For this type of function, it is easy to identify a choice of size parameters whereby most inhibition is delivered to the center of a circular target region than to the edges (simulations not shown). If this interpretation is correct, we predict that the spatial distribution of surround inhibition would strongly depend on the eccentricity and size of the target region. Preliminary evidence in this direction comes from our foveal data for which we did not observe significant anisotropies within the target region (although the lack of spatial specificity may be simply a consequence of insufficient data, see RESULTS for details). Further experiments will be necessary to pinpoint the origin of the spatial anisotropy we observed for the periphery.

GRANTS

This work was supported by National Eye Institute Grant RO1EY-0178 and by the Royal Society (University Research Fellowship) and Medical Research Council (New Investigator Research Grant).

REFERENCES

- Abbey CK, Eckstein MP.** Classification image analysis: estimation and statistical inference for two-alternative forced-choice experiments. *J Vision* 2: 66–78, 2002.
- Ahumada AJ Jr.** Classification image weights and internal noise level estimation. *J Vision* 2: 121–131, 2002.
- Allman J, Meizin F, McGuinness E.** Stimulus specific responses from beyond the classical receptive field: neurophysiological mechanisms for local-global comparisons in visual neurons. *Annu Rev Neurosci* 8: 407–430, 1985.
- Born RT.** Center-surround interactions in the middle temporal visual area of the owl monkey. *J Neurophysiol* 84: 2658–2669, 2000.
- Born RT, Bradley DC.** Structure and function of visual area MT. *Annu Rev Neurosci* 28: 157–189, 2005.
- Burgess AE, Colborne B.** Visual signal detection. IV. Observer inconsistency. *J Opt Soc Am A* 5: 617–627, 1988.
- Busse L, Katzner S, Tillmann C, Treue S.** Effects of attention on perceptual direction tuning curves in the human visual system. *J Vis* 8: 1–13, 2008.
- Cavanaugh JR, Bair W, Movshon JA.** Selectivity and spatial distribution of signals from the receptive field surround in macaque V1 neurons. *J Neurophysiol* 88: 2547–2556, 2002.
- Edwards M, Crane MF.** Motion streaks improve motion detection. *Vision Res* 47: 828–833, 2007.
- Falkenberg HK, Bex PJ.** Contextual modulation of the motion aftereffect. *J Exp Psych Hum Percept Perform* 33: 257–270, 2007.
- Levi DM.** Crowding—an essential bottleneck for object recognition: a mini-review. *Vision Res* 48: 635–54, 2008.
- McAdams CJ, Maunsell JH.** Effects of attention on orientation-tuning functions of single neurons in macaque cortical area V4. *J Neurosci* 19: 431–441, 1999.
- Murray RF, Bennett PJ, Sekuler AB.** Optimal methods for calculating classification images: weighted sums. *J Vis* 2: 79–104, 2002.
- Murray RF, Sekuler AB, Bennett PJ.** A linear cue combination framework for understanding selective attention. *J Vis* 3: 116–145, 2003.
- Neri P.** Spatial integration of optic flow signals in fly motion-sensitive neurons. *J Neurophysiol* 95: 1608–1619, 2006.
- Neri P, Levi DM.** Receptive versus perceptive fields from the reverse-correlation viewpoint. *Vision Res* 46: 2465–2474, 2006.
- Neri P, Levi DM.** Temporal dynamics of directional selectivity in human vision. *J Vision* 8: 1–11, 2008a.
- Neri P, Levi DM.** Evidence for joint encoding of motion and disparity in human visual perception. *J Neurophysiol* 100: 3117–3133, 2008b.
- Pack CC, Hunter JN, Born RT.** Contrast dependence of suppressive influences in cortical area MT of alert macaque. *J Neurophysiol* 93: 1809–1815, 2005.
- Paffen CLE, van der Smagt MJ, te Pas SF, Verstraten FAJ.** Center-surround inhibition and facilitation as a function of size and contrast at multiple levels of visual motion processing. *J Vision* 5: 571–578, 2005.
- Tadin D, Lappin JS, Gilroy LA, Blake R.** Perceptual consequences of centre-surround antagonism in visual motion processing. *Nature* 424: 312–315, 2003.
- Tadin D, Lappin JS, Blake R.** Fine temporal properties of center-surround interactions in motion revealed by reverse correlation. *J Neurosci* 26: 2614–2622, 2005.
- Treue S, Martínez-Trujillo JC.** Feature-based attention influences motion processing in macaque visual cortex. *Nature* 399: 575–579, 1999.